Temperature field measurement in titanium alloy during high strain rate loading - Adiabatic shear bands phenomenon

Nicolas Ranc, Laurent Tavarella, Vincent Pina, Philippe Hervé

Temperature field measurement in titanium alloy during high strain rate loading—Adiabatic shear bands phenomenon

N. Ranc [a,b,*], L. Taravella [c], V. Pina [a], P. Herve [a]

[a] L.E.E.E., E.A.387, Université de Paris X, Nanterre, 1, Chemin Desvallières, 92410 Ville d'Avray, France
[b] L.M.S.P., U.M.R. C.N.R.S. No. 8106, ENSAM – ESEM, 151, Boulevard de l'Hôpital, 75013 Paris, France Centre
[c] d'Expertises Parisien, DGA/DET, 16 Bis Avenue Prieur de la Côte d'Or, 94114 Arcueil Cedex, France

This paper concerns the study of the damage and failure mechanisms of metallic materials under dynamic loading. For high strain rates, it appears a strain localization in narrow bands called adiabatic shear bands (ASB). As the loading dura-tion is very short, the dissipation of the mechanical energy into heat generates strong temperature heterogeneities. To study the mechanisms of initiation and propagation of ASB during a dynamic torsion test, we developed an experimental device to measure temperature by pyrometry: for the "low temperatures" ranging between 50 °C and 300 °C, we use a bar of 32 InSb infrared detectors in order to study temperature heterogeneities during the ASB formation. The acquisition frequency is 1 MHz and the spatial resolution is 43 lm. For the "high temperatures" ranging between 800 °C and 1700 °C, we use an intensified camera whose spectral band is in the visible range. The spatial resolution is 2 lm and the aperture time is 10 ls. This device shows that the temperature could exceed 1100 °C with temperature heterogeneity inside the band. The "low temperatures" device allows us to observe the formation of one or two adiabatic shear bands on temperature recording along the torsion axis of the specimen. In order to explain these results, we propose a mechanism of multiple ASB formation followed by interactions and annihilations of the ASB.

Keywords: Adiabatic shear bands; Visible pyrometry; Infrared pyrometry; Multiple initiation; Localization

1. Introduction

Adiabatic shearing is a fracture mechanism generally observed in materials during dynamical loading. This phenomenon is characterized by a localization of the plastic deformation in narrow bands. Depending on materials, the width of these bands can vary between 10 and a few hundred micrometers.

The mechanisms of these adiabatic shear bands formation was first explained by Zener and Hollomon (1944): in metallic materials, a large proportion of the plastic deformation energy is converted into heat. During a dynamical loading, as the deformation duration is very short, the heat transfers by conduction in the material are negligible. That is why these shear bands are called adiabatic shear

* Corresponding author. Address: L.M.S.P., U.M.R. C.N.R.S. No. 8106, ENSAM – ESEM, 151, Boulevard de l'Hôpital, 75013 Paris, France. Tel.: +33 1 44 24 61 45; fax: +33 1 44 24 64 68.
E-mail address: nicolas.ranc@paris.ensam.fr (N. Ranc).

bands (ASB). The consequence of this effect is a local growth of the temperature in these bands (several hundreds of degrees Celsius), a thermal softening of the material and a local increase of the plastic deformation. This catastrophic process is characteristic of a plastic instability. However on the scale of the band, conduction is not negligible. In fact, the thermal properties and more precisely the thermal diffusivity determine the thickness of the band (Merzer, 1982). Generally, intense plastic shear strain in the band is the precursor of voids growth and crack initiation and propagation.

Many processes of fast metal forming generate adiabatic shear bands. The most characteristic examples are high speed machining (Molinari et al., 2002; Burns and Davies, 2002) and armour perforation by kinetic energy projectiles (Magness, 1992; Magness et al., 1995).

Since their discovery by Tresca (1878), the adiabatic shear bands always arouse a great deal of interest within the scientific community (Bai and Dodd, 1992 and Wright, 2002). However, in spite of many works on the subject, all the mechanisms of initiation and propagation are not completely known today. For example, concerning the experimental level, the design of a measurement device adapted to time and space scales of adiabatic shear bands remains a delicate work. The formation duration of an ASB is indeed about 10 μs and the band width is around 10 μm.

The ASB formation mechanism proposed by Zener and Holomon suggests that the temperature is a very interesting parameter in order to study the formation and the propagation of the adiabatic shear bands. Many experimental works were interested in the measurement of the temperature in the bands. Taking into account the low width of these bands and the speed of the phenomenon, pyrometry is an experimental technique particularly adapted to the temperature determination in an ASB. Moreover, in the last few years, the constant improvement of the performances of the detectors and of the associated optical systems allowed to increase the measurements precision as well as the space and temporal resolutions. The first pyrometric measurements used to understand mechanical properties of materials were carried out by Moss and Pond (1975). They used a germanium semiconductor doped with copper to measure the temperature variation at the surface of a copper specimen during elongation. Since 1979, Costin et al. have measured an increase in 100 °C inside an adiabatic shear band by using an InSb mono-detector of 1 mm in diameter. In 1987, Hartley et al. measured the temperature profile along the useful part of a torsion specimen with a bar of 10 photovoltaic InSb detectors. To limit the chromatic aberrations, the optical device is made up of a spherical mirror. It enables them to have two space resolutions of 20 μm and 250 μm. The tested materials are the 1018CRS steel (width of a band: 250 μm) and the 1020HRS steel (size of a band: 150 μm). The maximum increase in temperature is about 450 °C. In 1988, Marchand and Duffy used a bar of 12 InSb detectors with a Cassegrain optical device to limit the chromatic and spherical aberrations. With this device, they can visualize on the torsion specimen twelve zones of 35 μm by 35 μm and spaced of 11 μm. The maximum temperature reached 590 °C in a HY100 steel. This same experiment was also carried out later in 1992 by Duffy and Chi on various steels and in 1998 by Liao and Duffy on the titanium alloy Ti–6Al–4V. With a better space resolution (17 μm), the authors could measure maximum temperatures between 440 °C and 550 °C in Ti–6Al–4V. In 1996, Zhou et al. measured the temperature in an adiabatic shear band on the section of an impact loaded pre-notched plates at various speeds. The specimen materials were the Ti–6Al–4V and C300 steel. They used a bar of 16 InSb detectors of 80 μm by 80 μm. In the case of C300 steel, they observed intense heating over a width of around 200 μm. The heating amplitude depended on the impact speed and for a projectile speed of 40 ms^{-1}, the maximum temperature exceeded 1400 °C. In the case of the Ti–6Al–4V, the authors remarked that the heating was more diffuse and that the highest temperature was lower (about 450 °C for a projectile speed of 64 ms^{-1}). To limit the temperature error due to the uncertainties on the emissivity value, Pina developed in 1997 a new measurement device based on the monochromatic visible pyrometry (wavelength: 0.634 μm). The temperatures measured in titanium alloy Ti–6Al–4V reached 1300 °C during a punching test. The time and space resolutions are, respectively 5 μs and approximately 4 μm. A measurement in infrared spectral range (wavelength around 5 μm), more sensitive to the variation of the emissivity, enabled him to detect the α–β phase transition at the temperature of 996 °C. More recently, in 2001, Guduru et al. highlighted the two-dimensional character of the ASB by visualizing the temperature field at a distance of 5.5 mm of a crack point during the shear band formation. They used a matrix of 8×8

HgCdTe detectors coupled to an optical system with a magnification of 0.9. The observed zone of one detector on the specimen is an area of 110 μm per 110 μm and the refresh time of the camera is about 1 μs. They reported that the temperature distribution along the band is highly non-uniform with discrete regions of high temperature. The distance between two hot points varied between 250 μm and 1.0 mm.

The objective of these various works was primarily to evaluate the maximum temperature reached in fully formed adiabatic shear band (stage 3 suggested by Marchand and Duffy, 1988). The temperature measurement devices quickly developed thanks to the improved performance of the detection systems (optical device and detector). By studying the measured data of ASB temperature available in the literature, we can notice a relation between the value of the measured temperature and the spatial resolution of the thermal elements. When the space resolution increase, the measured temperature increase and the precision of measure increase. We can also note the difficulty to quantify the band temperature in titanium alloy Ti–6Al–4V, which can be explained by the fact that the bandwidths are almost 10 times lower in the Ti–6Al–4V than in steels. Apart from the works of Guduru et al. in 2001, the experimental devices used in the literature do not allow the quantification of the low temperatures (under 200 °C) corresponding to the beginning of the strain localization (stages 1 and 2 defined by Marchand and Duffy, 1988). The main difficulty of the low temperatures measurements is the weak level of the emitted signal.

The main objective of this paper is to better understand the strain and fracture mechanisms which predominate during a dynamic loading and in particular during the formation of adiabatic shear bands. To answer this question, we designed an experimental device which allows to accurately quantify the temperature field on the specimen surface during a dynamic loading. This system was adapted to the torsion Kolsky bars device classically used to form ASB. However, it is impossible to design one pyrometer which is able to detect a temperature range between 50 °C and 1670 °C (melting point of Ti–6Al–4V) with a sufficient precision. In this paper, we are thus particularly interested in two different temperature ranges:

The first, called ''low temperatures'', relates to temperature ranging between 50 °C and 300 °C. It corresponds to the onset of the plastic strain localization which occurs between 100 °C and 150 °C (transition from stage 1 to stage 2 defined by Marchand and Duffy). The objective is to detect temperature heterogeneities just before the localization which would likely generate an adiabatic shear band. Therefore, the ''low temperatures'' device requires a temporal resolution of about 1 μs. The difficulty associated with the low temperatures comes from the low level of the radiation emitted by the surface.

The second range, called ''high temperatures'' (temperatures between 800 °C and 1700 °C) will allow to quantify the maximum temperatures reached in a fully formed shear bands and perhaps to justify that the temperature inside the band is close to the melting point. In this study we have rather chosen to make only one measurement of the temperature field but with a very good spatial resolution (few microns). Moreover, for high temperatures and high plastic strains (high variations of the surface roughness), it is very difficult to quantify the evolution of the emissivity during a test. In order to limit the errors on the temperature determination related to the uncertainty on the emissivity, we chose a pyrometer whose spectral range is in the visible domain and thus less sensitive to the surface emissivity.

After this introduction, the first part of this paper will relate to the presentation of the temperature measurement system. In the second part, we will present and analyze the obtained results.

2. Experimental device

2.1. Material and specimen geometry

2.1.1. Material

The material used for the specimen is the titanium alloy Ti–6Al–4V. At room temperature, the Ti–6Al–4V whose composition is given in the Table 1, presents a biphasic structure αβ. The thermo mechanical treatment included an ironworks in the β field (temperature higher than 996 °C), a rolling in the αβ field (between 930 °C and 960 °C) and an annealing for 1 h at 790 °C, followed by a cooling in the furnace. Fig. 1 shows the transverse cross-section microstructure of this alloy. It is made of quasi equiaxed α grains (grain size between 5 and 10 microns) and β grains in minority around the α grains. We can also notice the presence of rolling bands in which the α grains have a very lengthened morphology (grains width near 3 or 4 microns).

Table 1
Chemical composition of the Ti–6Al–4V titanium alloy

Element	Al	V	O	C	N	Fe	Ti
Weight %	6.26	3.88	0.17	0.01	0.006	0.0017	89.67

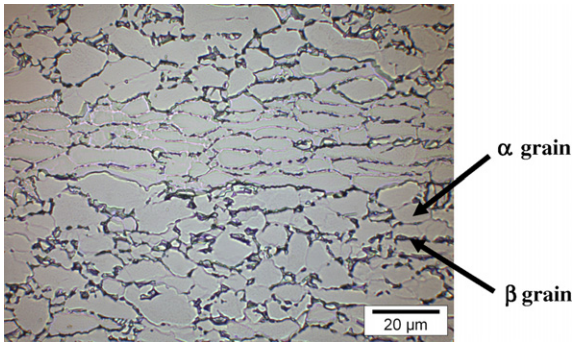

Fig. 1. Transverse cross-section microstructure of the titanium alloy Ti–6Al–4V.

2.1.2. Geometry of the specimen

The torsion specimen has a thin wall tubular geometry with two flanges for attachment to the loading device. This geometry is similar to that used by Marchand and Duffy (1988) and later by other authors (Deltort, 1994; Liao and Duffy, 1998). This type of specimen has the advantage of allowing the direct visualization of the ASB formation. However, the tubular part of the specimen has a small reduction of the section in its center in order to be certain that the shear band does not appear on the edges. Fig. 2a and b, respectively show a photograph and a plan of the torsion specimen. The thickness of the thin wall is 0.4 mm and the length of the tubular part is 2 mm. In order to have a good reproducability of the tests, we paid particular attention to the coaxiality of interior and external cylindrical surfaces which directly controls the thickness of the thin wall and to the roughness of various surfaces of the useful part.

2.2. Loading device

The dynamic tests were performed with the torsion Kolsky (split-Hopkinson) bar device. This technique enables to request dynamically and to determine the nominal shear strain and shear stress in the specimen. It was developed by Kolsky in 1949 and it was used by numerous authors to study the ASB (Hartley et al. in 1987, Marchand and Duffy in 1988, Deltort in 1994 and Liao and Duffy in 1998). In this paper, we will detail only briefly this technique. For more information, this experimental device is detailed in Hartley et al. (1987). The principle of this technique is based on the elastic wave propagation along two cylindrical bars in aluminium alloy (the input bar and the output bar). The diameter of the bars is 3 cm and their length is 3 m. The torsion specimen is fixed between these two bars.

Before the test, the input bar is subjected to a torque between the hydraulic engine and a brake (Fig. 3). The brake is released suddenly and a torsion loading pulse is propagated along the input bar. When it reaches the specimen, a part of the incident pulse is transmitted to the output bar and the

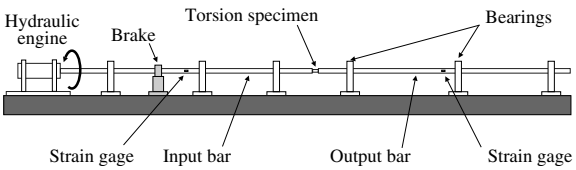

Fig. 3. Torsion Kolsky bar device.

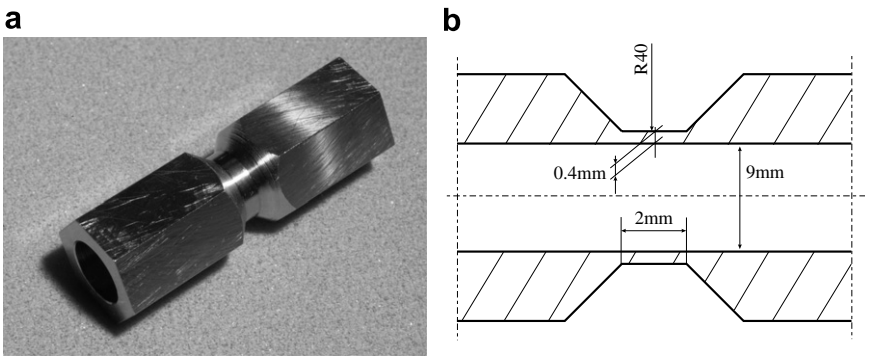

Fig. 2. Geometry of the torsion specimen (a) photograph of the specimen; (b) plan of the useful part.

other is reflected in the input bar. The shear strain induced by the loading pulse is measured by strain gauges placed in the centre of the bars. As shown by Kolsky in 1949, these time evolutions of strain allow to determine the average shear stress and the nominal shear strain of the specimen.

2.3. Temperature field measurement device

2.3.1. Pyrometry technique

To quantify the temperature during the ASB formation, we chose a measurement technique by pyrometry. The principle of this technique consists of determining a surface temperature from the measurement of its emitted energy. The pyrometry technique has many advantages: firstly, it is a non-intrusive measurement technique which does not disturb the temperature field on the surface. Secondly, this technique has a very short response time (in our case lower than a microsecond). Finally, it allows to visualize temperature cartographies with very good space resolution (lower than 10 μm). The design of a pyrometer consists of choosing a spectral range, which is linked to the measured temperature and the spectral sensitivity of the selected detector. The pyrometry technique and the various selection criteria of the detectors are detailed by Ranc et al. in 2004 and Ranc in 2004.

The energy emitted by a black body surface (perfect emitter) presents a maximum for a wavelength λ_{max}. For "low temperatures" (200 °C) and for "high temperatures" (1000 °C) this maximum is in the near infrared domain, respectively for the wavelengths of 6 μm and 2 μm. In pyrometry, another significant quantity is the radiance sensitivity to the temperature variations. It is characterized by the ratio $1/I^0_\lambda \partial I^0_\lambda/\partial T$ where I^0_λ is the spectral intensity defined as the power radiated by a unit surface in a direction $\boldsymbol{\delta}$ and in a solid angle of one steradian. For a black body, the sensitivity is higher when the wavelength decreases. So, to increase the sensitivity of a pyrometer, it is necessary to choose the smallest possible wavelength. The choice of the spectral range of the pyrometer is thus a compromise between the lowest possible wavelength and a sufficient emitted energy which can be detected. In this study, for the "low temperatures" range, we chose an InSb infrared detector (between 1 μm and 5.5 μm) and for the "high temperatures" range, we chose a intensified CCD camera whose spectral band is in the visible range (between 0.4 μm and 0.8 μm).

The radiative behavior of a real surface is different from a black body's. The spectral emissivity is defined as the ratio between the spectral intensity of the real surface and the spectral intensity of a black body in the same temperature. Its value lies between 0 and 1. The emissivity is a thermo-optical property of the surface which depends on the material (Palik, 1985), the surface roughness (Hervé, 1977), the physical state of material (solid–liquid) (Antoni Zdziobek et al., 1997), the surface temperature (Piriou, 1973), the direction of emission (Birkebak and Eckert, 1965) and the wavelength (Hiernaut et al., 1986).

The main error during a temperature measurement by pyrometry is related to uncertainty on the emissivity value of the surface. During the mechanical loading, the plastic deformation modifies the roughness of the specimen surface and its temperature and therefore the emissivity. If we make the assumption that the surface behaves like a black body so that its emissivity is equal to 1, we obtain the radiance temperature noted T_λ. Fig. 4 represents the difference between the radiance temperature and the real temperature according to the real surface temperature. On this graph, the emissivity is supposed to be constant in the sensitivity range of each pyrometer and is estimated from bibliographical data bases (Touloukian and DeWitt, 1970). In near infrared and visible ranges, the emissivity values were, respectively taken equal to 0.25 and 0.4. For a temperature of 200 °C in the infrared range, the error on temperature is 81 °C and the corresponding relative error is 17%. A variation of 10% of the emissivity value causes, respectively an error of 5 °C (1%). For a temperature of 1000 °C in the visible range, the error is 70 °C (relative error of 6%).

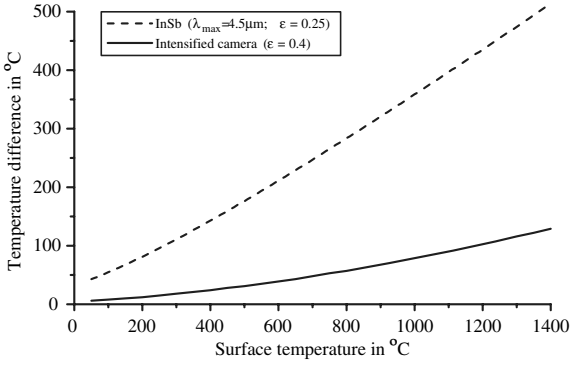

Fig. 4. Difference between the radiance temperature and the real temperature for an InSb detector and an intensified camera.

An emissivity variation of 10% causes an error of 8 °C (0.6%).

2.3.2. Measurement of the emissivity in the infrared range

The error obtained in the "low temperatures" range is too significant. To limit these errors in the infrared range, the emissivity was measured in a temperature range between 75 °C and 350 °C and for different surface roughness. These measurements are taken on a square specimen of 5 cm dimension and 2 mm thickness. A half of the specimen was painted with a strongly emissive black paint. This zone is used as a black body reference. The other half is made up of Ti–6Al–4V with three different roughnesses: the first corresponds to a polished mirror ($Ra = 0.021$ μm), the second a machining roughness identical to the torsion specimen ($Ra = 0.297$ μm) and the third a frosted surface ($Ra = 0.869$ μm). The specimen is fixed on a heater and placed in a chamber. Its temperature is measured by a thermocouple. The comparison between the photovoltaic InSb detector signal corresponding to the painted part and the unpainted part allows to determine the emissivity associated with the InSb detector spectrum noted $\varepsilon_{\mathrm{nSb}}$. We can write the relation between this emissivity and the monochromatic emissivity:

$$\varepsilon_{\mathrm{InSb}} = \frac{\int_{\lambda_1}^{\lambda_2} \varepsilon(\lambda, T)\eta(\lambda)L_{\lambda}^{0}(\lambda, T)\mathrm{d}\lambda}{\int_{\lambda_1}^{\lambda_2} \eta(\lambda)L_{\lambda}^{0}(\lambda, T)\mathrm{d}\lambda} \quad (1)$$

With η the detector efficiency, λ_1 and λ_2, wavelength range of the detector sensitivity.

The emissivity measured by this experimental device takes into account the reflexion on the sample of the thermal radiation of the chamber at ambient temperature (Fig. 5). It is thus about an apparent emissivity. In the experimental configuration associated to adiabatic shear bands, this reflexion of the environment at ambient temperature on the specimen is also present. The temperature evaluation during a torsion loading must, therefore, use this apparent emissivity. The apparent emissivity of Ti–6Al–4V is given in Fig. 6 for different roughness.

To check that the surface does not oxidize, we carried out a cycle of rise followed by a descent of the surface temperature. The emissivities measured in the rise and in the descent are appreciably equal. Oxidation does not occur in our temperature range and for our test duration. Fig. 6 shows that the

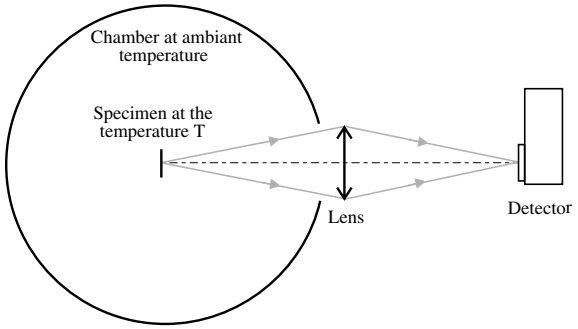

Fig. 5. Experimental device to measure emissivity for the "low temperatures" range in the near infrared spectral range.

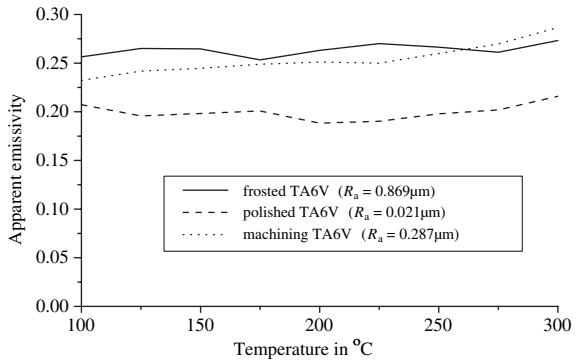

Fig. 6. Apparent emissivity evolution according to the temperature and the surface roughness.

apparent emissivity varies a little with the temperature in our studied temperature range. During the plastic deformation, the surface roughness increases (transition from a machined state to a rough state). The experimental data show that the apparent emissivity vary a little for these two surface qualities. For dynamical torsion tests, we will take it equal to 0.25 ± 0.025. This uncertainty on the emissivity corresponds to an error on temperature 4 °C for a surface temperature of 50 °C (relative error: 1%) and 10 °C for a surface temperature of 280 °C (relative error: 2%).

2.3.3. Experimental device associated with the study of adiabatic shear bands

For the "low temperatures" range, we use a bar of 32 photovoltaic InSb detectors which is cooled with liquid nitrogen. The detectors are coupled with a unit magnification optical system made up of two parabolic mirrors in order to limit chromatic and geometrical aberrations. The focal length of the two mirrors is 152 mm. The spectral range of the detectors are in the infrared range (wavelengths

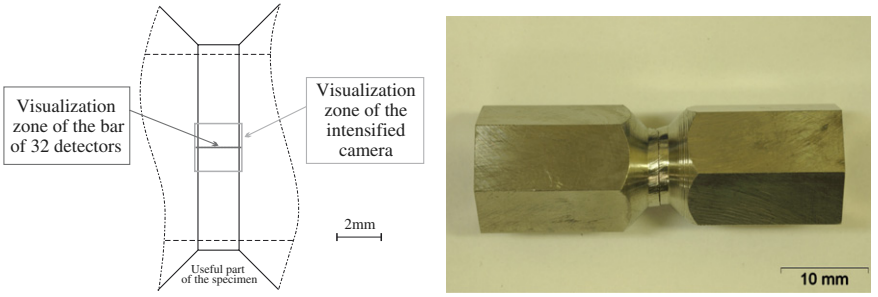

Fig. 7. Visualization zones of the bar of InSb detectors and the intensified camera on the useful part of the specimen.

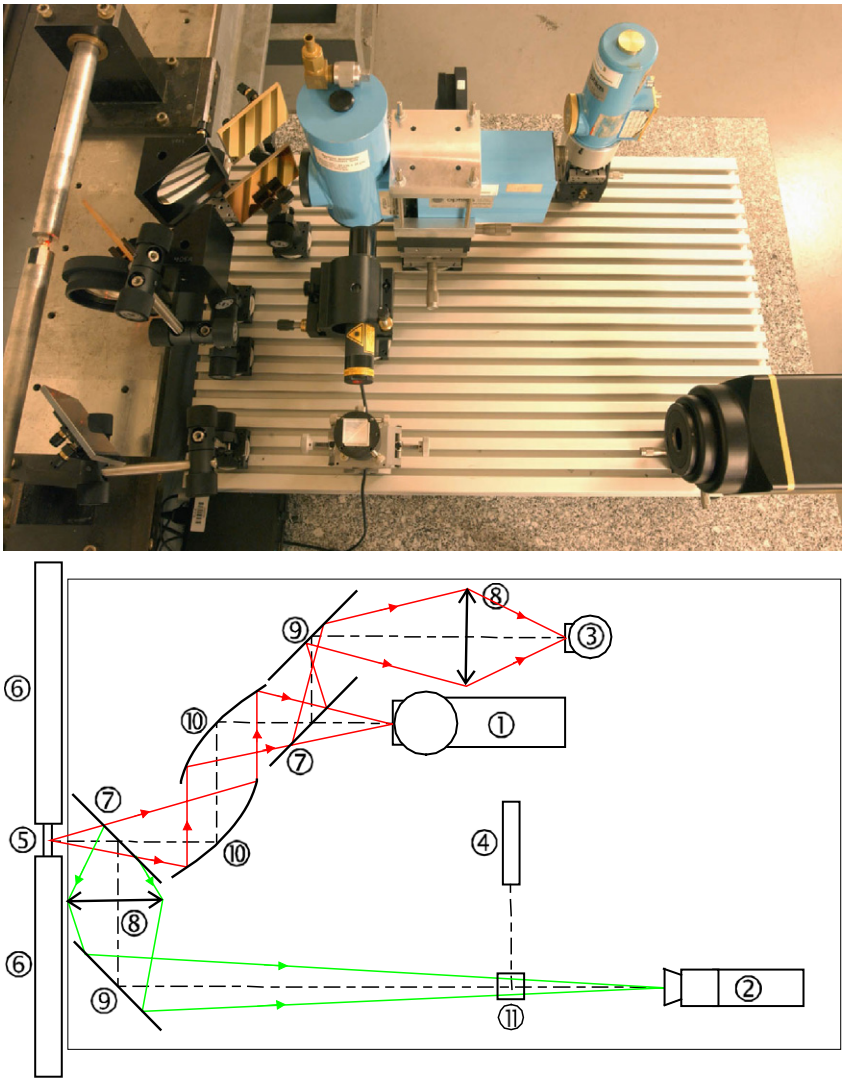

(1) bar of 32 InSb detectors, (2) intensified camera, (3) InSb mono-detector, (4) alignment laser, (5) torsion specimen, (6) input and output bars, (7) dichroic and beamsplitter plates, (8) glass lens, (9) plane mirrors, (10) parabolic mirrors, (11) beamsplitter cube

Fig. 8. Experimental device to measure temperature.

between 1 μm and 5.5 μm). The size of the detectors is 43 μm by 43 μm and their response time is 500 ns. The space between two detectors is 18 μm and the total length is 1.934 mm. The visualized zone on the specimen is represented in Fig. 7. Each detector output signal is amplified and recorded by a data acquisition system with a sampling rate of 1 MHz. In order to correlate the strain, the stress and the temperature evolutions, we use the same temporal reference for the data acquisition.

For the "high temperatures" range, we use a 16 bit numerical intensified CCD camera with a GaAs photocathode. Its spectral band is located in the visible range between 0.4 μm and 0.8 μm wavelengths. The energy radiated by the specimen is focused on the camera using a glass lens with a focal length of 100 mm. The magnification of the optical system is about 5. The observation field of the camera (around 2 mm × 2 mm) is given on Fig. 7. The total pixel number of the camera is about 1024 × 1024. Thus a pixel corresponds to a zone of 2 μm by 2 μm on the torsion specimen. The aperture times of the camera vary between 10 μs and 20 μs. During a dynamic torsion test, we carried out only one image because the refresh time of the CCD (100 Hz) is much larger than the ASB formation duration.

As the ASB formation duration is very short (a few tens of microseconds), it is difficult to precisely release the opening of the intensified camera. To solve this problem, we chose to trigger the camera from an InSb photovoltaic mono-detector signal which visualizes the totality of the useful part of the specimen (size of the observation zone: 2 mm by 2 mm). This detector allows to detect a significant increase in the temperature on the useful part of the specimen and to give a temporal reference in order to trigger the camera. The response time of the detector is about 500 ns, which allows a sufficiently precise release.

In order to align the various detectors on the centre of the useful part of the specimen, we use an alignment HeNe laser. A general scheme of the optical device is given in Fig. 8.

The pyrometers are calibrated on two black bodies, one for the "low temperatures" (manufacturer: Minirad System Inc.; model RBB-1000; precision between 2 °C and 3 °C; emissivity: 0.98 ± 1%), the other for the "high temperatures" (manufacturer: Pyrox; precision between 2 °C and 3 °C; emissivity: 0.99 ± 1%). The calibration curves are given in Fig. 9a and b.

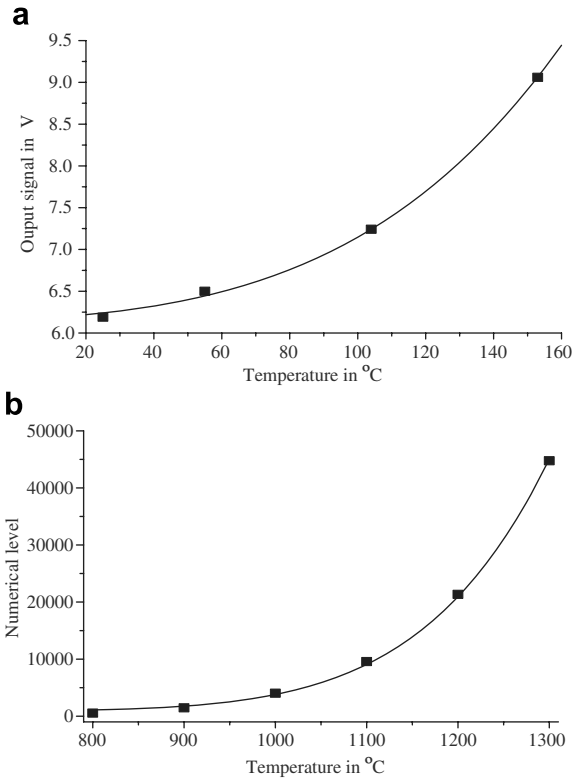

Fig. 9. Calibration curves according to the black body temperature. (a) InSb detector: "low temperatures" range; (b) intensified camera (aperture time: 10 μs): "high temperatures" range.

3. Results and discussion

3.1. General results

A series of 21 tests were carried out. Table 2 sums up these different tests and gives the associated nominal strain rate. Figs. 10 and 11 show the "low temperatures" results obtained during the dynamic test of torsion T19 at a nominal strain rate of 1920 s^{-1}. Fig. 10 represents the simultaneous evolution of the temperature measured in the centre of the adiabatic shear band and the average shear stress according to the nominal shear strain of the specimen. At the beginning of the test (stage 1), we note a quasi linear increase in the temperature with the nominal shear strain (approximately 0.5 K/μs). The yield stress then remains quasi constant equal to approximately 700 MPa. From a nominal deformation of a little more than 50%, the flow stress begins to drop rapidly and a very fast increase in the temperature between 10 K/μs and 15 K/μs (stage 2) appears. It corresponds to the formation of an adiabatic shear band. The temperature at the beginning of this stage

Table 2
Dynamic torsion tests

Test reference	Strain rate in s^{-1}
T1	1020
T2	1330
T3	1180
T4	1060
T5	1300
T6	1320
T7	1310
T8	1510
T9	1810
T10	1500
T11	1480
T12	1100
T13	1930
T14	1390
T15	1410
T16	1850
T17	1730
T18	1940
T19	1920
T20	2040
T21	2020

is approximately 130 °C. Fig. 11 represents the temperature variation measured by the bar of 32 InSb detectors (infrared range) according to time and the axial position on the specimen. The detector saturates for a temperature higher than 280 °C because this measurement device was designed only for low temperatures. We can notice that stage 1 corresponds to a domain of homogeneous temperature and thus of homogeneous plastic deformation whereas stage 2 highlights a strong temperature heterogeneity.

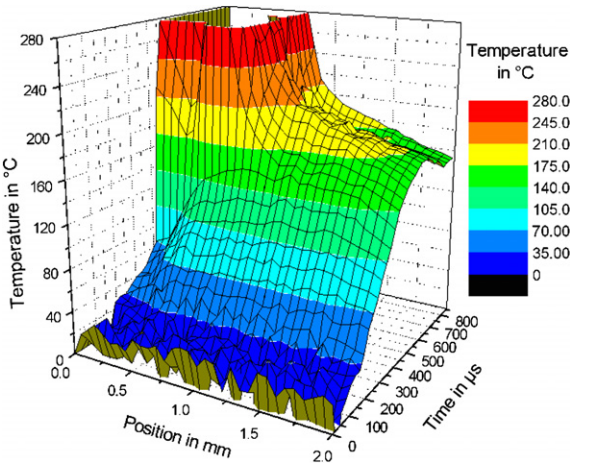

Fig. 11. Temperature heterogeneity on the specimen surface during T19 test (bar of InSb detectors).

The intensified camera is released from a threshold on the InSb detector signal with a delay of 40 µs. The aperture time of the camera is 10 µs. The signal of the InSb detector and the opening of the camera are represented in Fig. 12 according to time and the nominal shear deformation. The thermography obtained by the intensified camera is given in Fig. 13. The dotted line corresponds to the visualization zone of the bar of 32 detectors. The maximum radiance temperature is about 1000 °C. If we suppose that the emissivity in the visible field is about 0.4, the difference between the radiance and the real temperature is 80 °C (relative variation of 6%). The real temperature would then be 1080 °C.

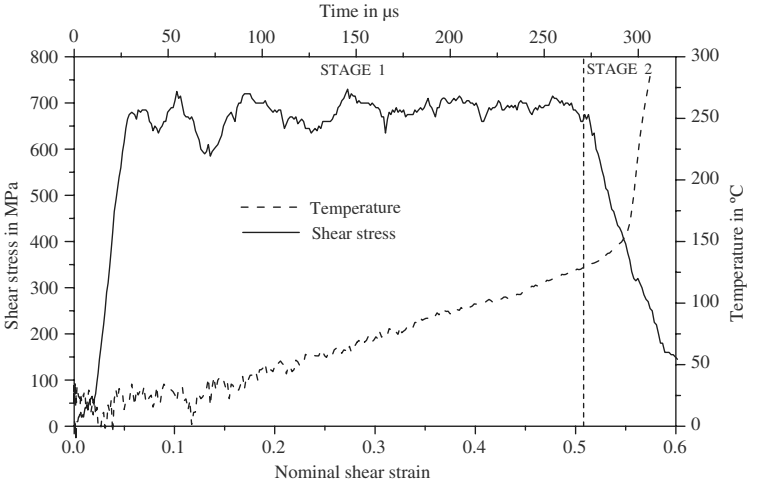

Fig. 10. Stress and temperature evolution during T19 test.

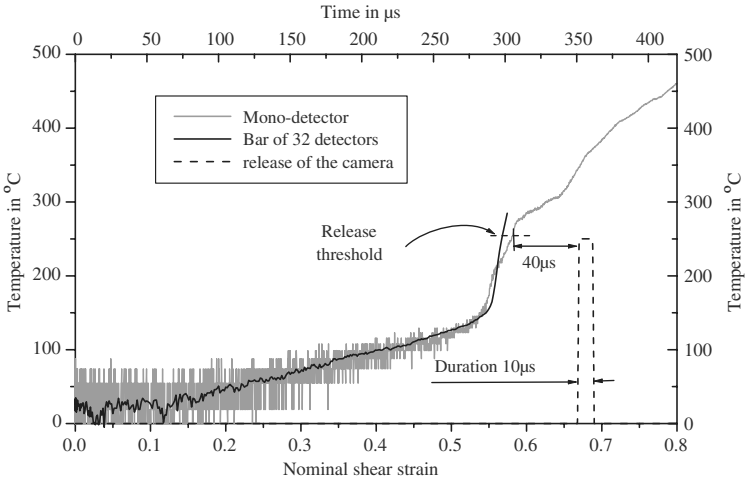

Fig. 12. Release of the intensified camera (T19 test).

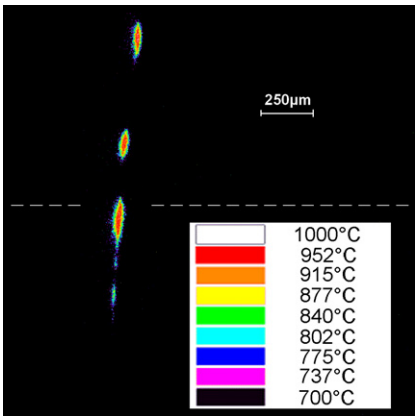

Fig. 13. Radiance temperature field during adiabatic shear band propagation (T19 test, aperture time: 10 µs).

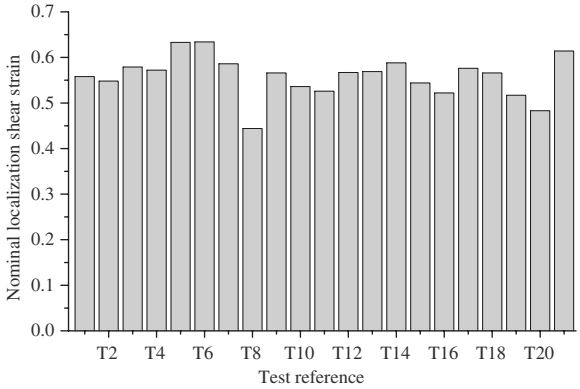

Fig. 14. Nominal localization strain; dispersion of the experimental values.

3.2. Adiabatic shear band initiation

3.2.1. Nominal localization strain

We can define the nominal localization shear strain as the nominal shear strain corresponding to a drop of 10% of the average shear stress. During various dynamic torsion tests of dynamic torsion, we can notice a small dispersion in the nominal localization strain value (Fig. 14). The average of the nominal localization strain is 0.56 with a standard deviation of 0.04.

3.2.2. Multiple initiations of adiabatic shear bands

A metallographic observation after the test always reveals the presence of only one ASB which extends only 80–90% around the specimen circumference. During the dynamic tests, we can sometimes observe a homogeneous temperature field because our experimental device visualizes only one side of the useful part of the specimen. In the other cases, we can observe at the localization onset time the formation of one or two adiabatic shear bands on temperature recording along the axis of the specimen. Figs. 15 and 16 show the observation of a single ASB in the visualized zone by the bar of 32 detectors during the test T4. On the contrary, we can notice during test T17 the formation of a first band in the center of the useful part of the specimen and a second on the left of the specimen a few tens of microseconds later (Fig. 17). We can even notice in Fig. 17 the presence of a third incipient band on the right part of the specimen which stops quickly. It is thus highly probable that several ASB start

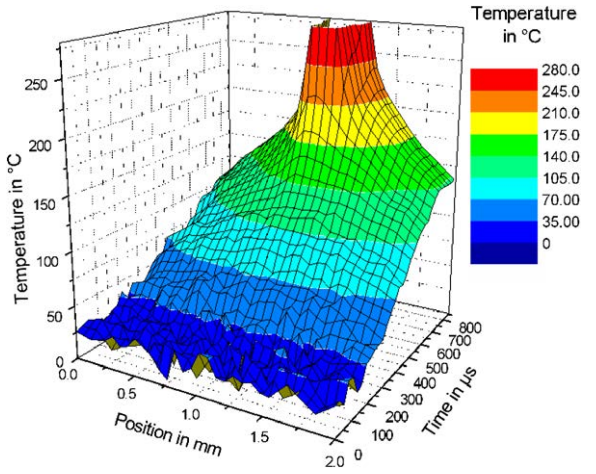

Fig. 15. Initiation of one shear band: T4 test (3D temperature visualization).

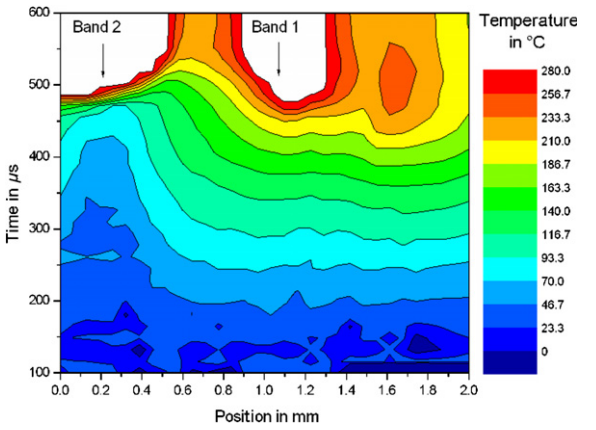

Fig. 17. Initiation of two shear bands: T17 test (2D temperature visualization).

simultaneously. In Fig. 17, the distance between the band 1 and the band 2 is about 1 mm. The order of magnitude of this value is in good agreement with the band spacing measured by Xue et al. (2002) during a radial collapse of a thick-walled cylinder test. In the case of the titanium alloy Ti–6Al–4V, the authors estimated a shear band spacing of 0.53 mm.

3.2.3. Delay between the increase in temperature and the stress drop

We can note during the dynamic torsion tests the presence of a temporal shift between the stress drop at the onset of the localization and the fast increase in the temperature in the ASB center. The tests T14 and T17, respectively highlight a delay of 2 µs (Fig. 18a) and 44 µs (Fig. 18b). The graphic in Fig. 19 shows the delay measured on all of the tests carried out. The delay cannot be given when the band occurs on the opposite side of the observation zone. The value of 44 µs represents the maximum measured delay for all performed tests. In Fig. 19, we write down the number of observed bands for each test. This temporal shift can be explained by the fact that a band starts on the opposite of the observed side and propagates all around the specimen before being observed by the bar of InSb detectors. A delay of 60 µs was already measured by Marchand and Duffy in a HY100 steel (1988).

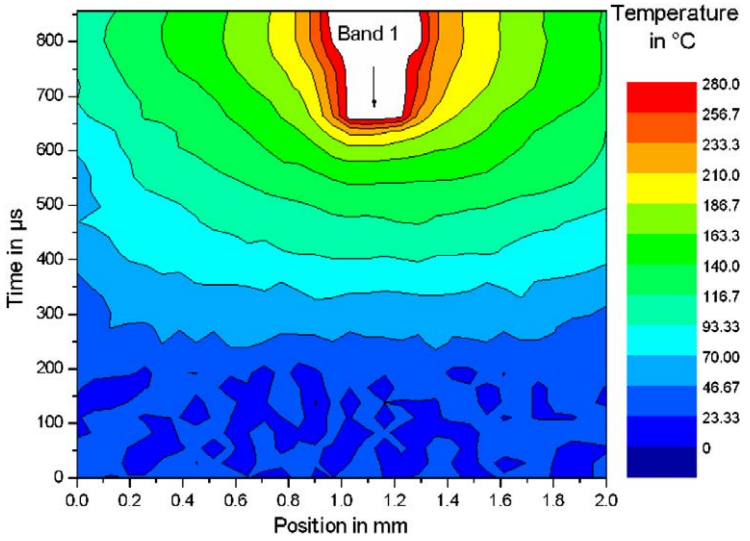

Fig. 16. Initiation of one shear band: T4 test (2D temperature visualization).

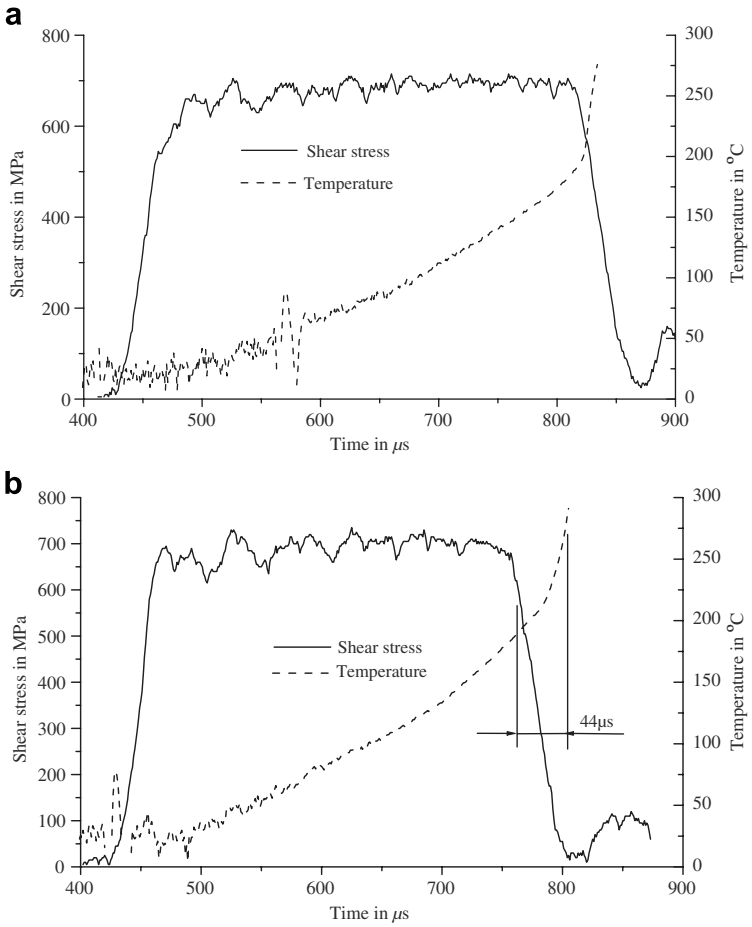

Fig. 18. Delay between the average stress drop and the increase in temperature: (a) T14 test; (b) T17 test.

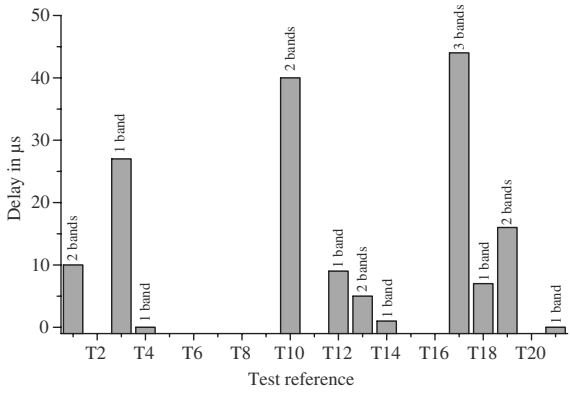

Fig. 19. Measurements of the delay for the different tests.

3.2.4. Proposition of a nucleation mechanism of the ASB

In their experimental study, Marchand and Duffy (1988) noted that at the same moment, the bands are not all formed necessarily in the same normal plan to the torsion axis direction and that the local plastic deformation in the band is very heterogeneous around the specimen. To explain these results they proposed two different mechanisms of band formation. In the first case, the ASB formation would break up into a stage of bands nucleation at various places around the circumference of the specimen at the same moment and a stage of growth and coalescence of nuclei in order to form only one band around the specimen; the second possible mechanism would be characterized by the formation of only one band in a point of the specimen circumference followed by its propagation around the specimen. The fact that the bands are not in the same plan supports the first mechanism whereas a great disparity of the plastic strain around the specimen would support the second mechanism. However, today still many questions remain concerning the existence of these mechanisms.

Our experimental observations in the "low temperatures" range show that several bands can start on the useful part of the specimen. On the other hand, the metallographic post-mortem observations and thermographies of the bands in the final phase ("high temperatures" range) reveal on the contrary always only one band. We can thus think that there is an interaction between its incipient bands which leads to the annihilation of a great number of initiate ASB. Moreover, the existence of a delay between the stress drop and the fast increase in the temperature in the center of ASB shows that at least only one band can propagate on almost the totality of the specimen circumference. The interaction between ASB was already investigated in 1998 by Nesterenko et al. through the radial collapse of a thick-walled cylinder under high strain rate. In 2002, Xue et al. suggested a new model for ASB initiation and propagation based on the deactivation of ASB embryos. In a similar way, we can explain our experimental results with a mechanism of ASB initiation and evolution which break up into two stages:

- In the first stage: several ASB initiate simultaneously at various places in the useful part of the specimen and begin to grow in an independent way.
- In the second stage: when the plastic strain increases, the first band which will start to propagate will create a stress relaxation (stress drop) which extends all around the specimen. At the end, this first band will deactivate all the other incipient bands and propagate along the circumference of the specimen.

In graph 19 we can also notice that generally for a weak delay, we always observes the initiation of only one band. On the other hand for a delay close to the maximum (44 μs), it is likely that we can observe the initiation of several bands. This can be explained by the fact that the band which will deactivate all the other bands starts on the opposite side of the specimen. This observation thus supports the mechanism which we presented previously.

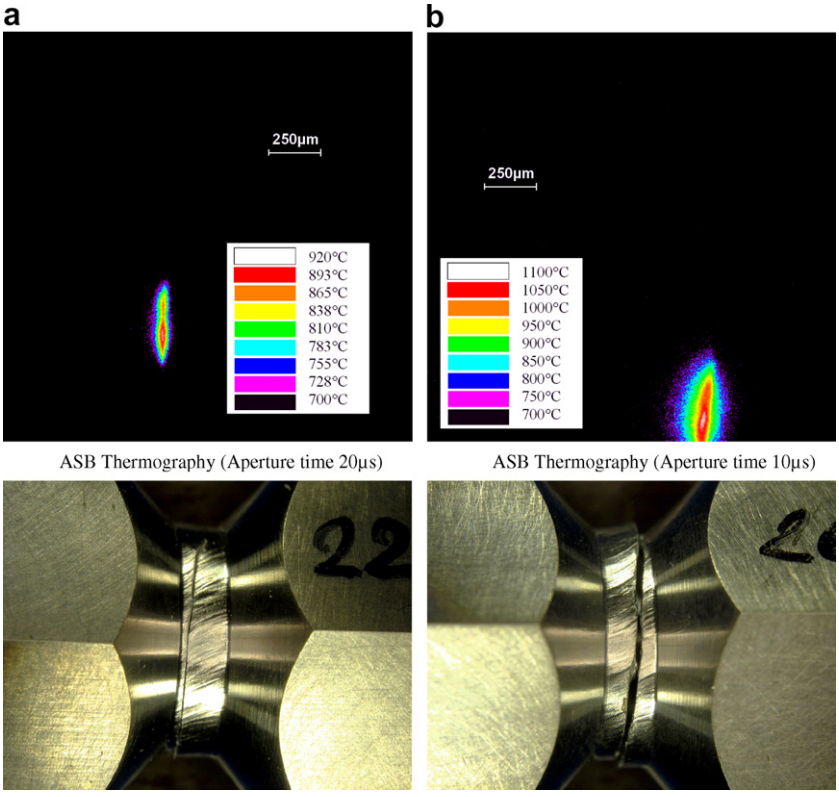

Fig. 20. Adiabatic shear band thermographies during dynamic torsion tests. (a) T1 test and (b) T13 test.

3.3. Maximal temperature inside ASB

Fig. 20 shows two thermographies of ASB at the propagation stage. For each test, the evolution of the stress, the temperature measured by one of the 32 InSb detectors located at the center of the ASB as well as the camera opening are given in Fig. 21.

The maximum temperatures inside the band are about 1000 °C and 1100 °C, respectively for the tests T1 and T13. They are higher than those measured by Zhou et al. in 1996 and Liao and Duffy in 1998 the Ti–6Al–4V but remain lower than that measured by Pina in 1997 and our previous work on a dynamic punching device (Ranc et al., 2000). Taking into account the uncertainties on the precision of the release of the camera starting from the InSb detector signal, it was difficult to control the duration between the stress drop and the camera opening. This can explain why we do not measure the maximum temperature reached inside the ASB. We can also wonder whether the temperature is stationary during the opening time of 10 μs or 20 μs. If it is not the case, the real temperature would be obviously higher.

However, for opening times of about 10 μs, the band does not seem like a continuous line but rather one hot point or a series of hot points on thermographies (see also Fig. 13). During the test T19, the distance between two hot points can be estimated between 250 μm and 300 μm. Two explanations of this phenomenon can be given to understand the formation of these hot points on thermographies: first these observations can be explained by the void nucleation and growth inside the fully formed adiabatic shear band. These voids were already observed by various authors (Bai et al. in 1993 and Xue et al. in 2002) in a post-mor-

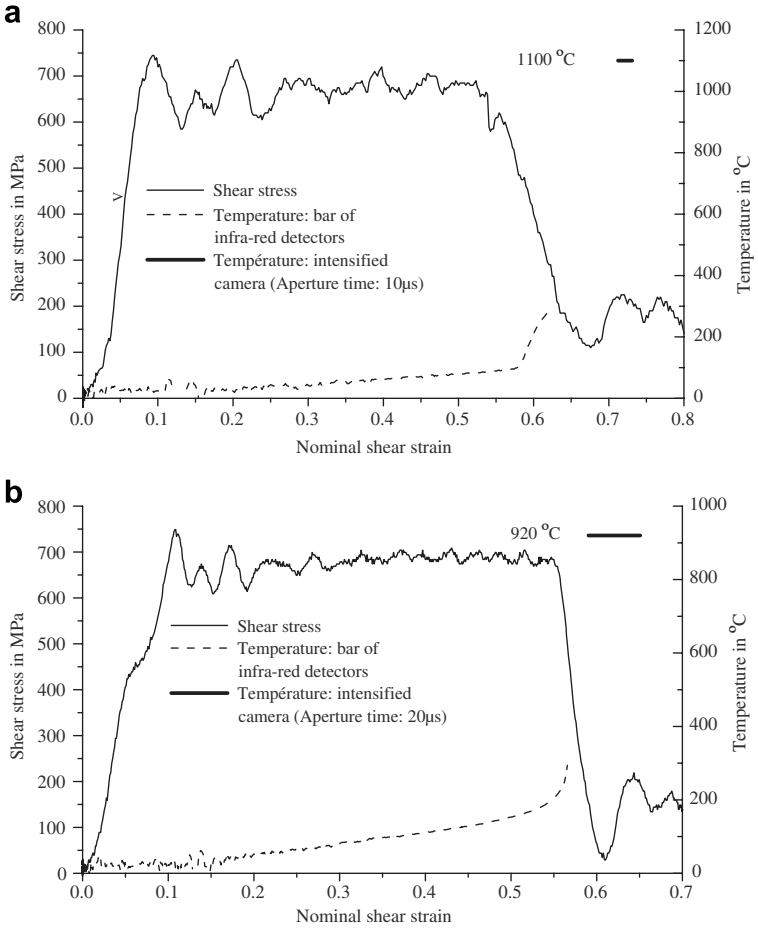

Fig. 21. Temperatures measurements (low and high temperature ranges). (a) T1 test and (b) T13 test.

tem microstructural characterization of ASB in the same titanium alloy. The second explanation is based on the fact that at the observation time, a crack is already formed along the shear band and the friction at the contact zone on the crack surfaces creates a series of hot points. However the second explanation seems less probable because the normal stress on the crack surface is very weak (or equal to zero) and thus the energy dissipated into heat and the temperature variations associated with this phenomenon remain weak. Moreover, the relative displacement of the crack tips remains also weak.

4. Conclusion

To study the initiation and propagation mechanisms of adiabatic shear bands, we developed an experimental device to measure temperature by pyrometry. We are more particularly interested in two ranges of temperature: one of the originalities of this work was to design a device which allows the detection of temperatures ranging between 50 °C and 300 °C (called "low temperatures" range) in order to study the ASB initiation and in particular temperature heterogeneities just before initiation. In addition, to study the ASB propagation stage and to quantify the maximum temperatures reached in the center of the band, we developed a pyrometer able to measure temperatures ranging between 800 °C and 1700 °C ("high temperatures" ranges) with a spatial resolution lower than the ASB size (a few tens of micrometers in Ti–6Al–4V alloy).

The main difficulties of the design of our measurement system are primarily related to the band size (a few hundred micrometers in the initiation stage and a few tens of micrometers in the propagation stage) and to the duration of ASB formation which is about 50 μs. For the low temperatures, the space resolution is 43 μm and the acquisition frequency is 1 MHz. Taking into account the low energy levels to be detected, the optical device was optimized to collect the maximum of the radiated flux. Measurement is taken in the near infrared field for wavelengths ranging between 1 μm and 5.5 μm with a bar to 32 InSb photovoltaic detectors.

For the "high temperatures" range, the space resolution is 2 μm. As the radiated power is more significant, we chose an intensified CCD camera whose visible spectral range between the wavelengths 0.4 μm and 0.8 μm. The aperture time of the intensified camera is 10 μs or 20 μs. Its release is carried out from the signal delivered by an InSb mono-detector detecting an increase in temperature on the totality of the zone visualized by the camera.

Another difficulty of the pyrometry technique is related to the uncertainties on the emissivity. The emissivity can depend on the surface temperature, of the surface roughness, and the possible phase transitions. For the low temperatures, the emissivity was measured in the case of a Ti–6Al–4V alloy for temperatures ranging between 75 °C and 300 °C and for various surface roughnesses. The results showed a weak variation of the emissivity in our temperature and roughness ranges. Thus, the emissivity will be supposed to be constant during the dynamic tests. For the high temperatures, one of the originalities of this work is to choose shortest possible wavelengths in order to limit the error due to uncertainty on the emissivity.

The experimental device of temperature measurement was then tested on a dynamic torsion test of torsion on the torsion Kolsky bars. The specimen has a tubular geometry with a small reduction of the section in the center of the useful part. Strain rates of the tests are between $1000\,s^{-1}$ and $2000\,s^{-1}$. The "low temperature" device allows to observe two stages: a first stage where the temperature remains homogeneous and a second stage where the temperature increases very quickly only inside the band. On the other hand, the intensified camera enabled us to quantify maximum temperatures inside the band reaching 1100 °C. Thermographies show heterogeneities of temperature in the center of the band which characterize the void nucleation and growth inside the shear band.

Measurements in the "low temperatures" range showed that according to the tests, it is possible to observe the initiation of one or two adiabatic shear bands. It is thus highly probable that several ASB initiate simultaneously. However the metallographic observations after tests always show the presence of only one fully formed band around the circumference of the specimen.

To explain these results, we used the following initiation mechanism: several ASB will start simultaneously and begin to grow in an independent way. When one ASB begin to propagate, it will create a stress relaxation (stress drop) and will deactivate some other started bands. At the end, only one band will deactivate all the other incipient

bands and propagate along all the circumference of the specimen.

References

Antoni Zdziobek, A., Pina, V., Hervé, P., Durand, F., 1997. A radiative thermal analysis method for phase change determination of strictly controlled refractory alloys. High Temp Mater Sci 37, 97–114.

Bai, Y., Dodd, B., 1992. Adiabatic Shear Localization – Occurrence, Theories and Applications. Pergamon Press, Oxford.

Bai, Y., Xue, Q., Xu, Y., Shen, L., 1994. Characteristics and microstructure in the evolution of shear localization in Ti–6Al–4V alloy. Mech. Mat. 17, 155–164.

Birkebak, R.C., Eckert, E.R.G., 1965. Effects of roughness of metal surfaces on angular distribution of monochromatic reflected radiation. ASME J Heat Transfer 87, 85–94.

Burns, T.J., Davies, M.A., 2002. On repeated adiabatic shear band formation during high speed machining. Int. J. Plast. 18, 487–506.

Costin, L.S., Crisman, E.E., Hawley R.H., Duffy, J., 1979. On the localisation of plastic flow in mild steel tubes under dynamic torsional loading. In: Harding, J. (Ed.), Proceedings of the 2nd Conference on the Mechanical Properties of Materials at High Rates of Strain. The Institute of Physics, London, pp. 90–100.

Deltort, B., 1994. Experimental and numerical aspects of adiabatic shear in a 4340 steel. J. Phys. IV C8, 447–452.

Duffy, J., Chi, Y.C., 1992. On the measurement of local strain and temperature during the formation of adiabatic shear bands. Mater. Sci. Eng. A 157, 195–210.

Guduru, P.R., Ravichandran, G., Rosakis, A.J., 2001. Observation of transient high temperature vortical microstructures in solids during adiabatic shear banding. Phys. Rev. E 64, 1–6.

Guduru, P.R., Rosakis, A.J., Ravichandran, G., 2001. Dynamic shear bands: an investigation using high speed optical and infrared diagnostics. Mech. Mat. 33, 371–402.

Hartley, K.A., Duffy, J., Hawley, R.H., 1987. Measurement of the temperature profile during shear band formation in steels deforming at high strain rates. J. Mech. Phys. Solids 35 (3), 283–301.

Hervé, P., 1977. Influence de l'état de surface sur le rayonnement thermique des matériaux solides. Ph.D. Thesis. Paris VI.

Hiernaut, J.P., Beukers, R., Hoch, M., Matsui, T., Ohse, R.W., 1986. Determination of the melting point and of the spectral and total emissivities of tungsten, tantalum and molybdenum in the solid and liquid states with a six-wavelength. High Temp. High Press. 18, 627–633.

Kolsky, H., 1949. An investigation of the mechanical properties of materials at very high rates of loading. Proc. Phys. Soc. London B 62, 676–700.

Liao, S.C., Duffy, J., 1998. Adiabatic shear bands in a Ti–6Al–4V titanium alloy. J. Mech. Phys. Solids 46 (11), 2201–2231.

Magness, L.S., 1992. Properties and performance of kinetic energy penetrator materials. In: Bose A., Dowding, R.J. (Eds), Tungsten and Tungsten Alloys, pp. 15–22.

Magness, L.S., Kapoor, D., Dowding, R., 1995. Novel flow-softening and flow anisotropy approaches to developing improved tungsten kinetic energy penetrator materials. Materials and Manufacturing Processes 10 (3), 531–540.

Marchand, A., Duffy, J., 1988. An experimental study of the formation process of adiabatic shear bands in a structural steel. J. Mech. Phys. Solids 36 (3), 251–283.

Merzer, A.M., 1982. Modelling of adiabatic shear band development from small imperfection. J. Mech. Phys. Solids 30 (5), 323–338.

Molinari, A., Musquar, C., Sutter, G., 2002. Adiabatic shear banding in high speed machining of Ti–6Al–4V: experiments and modelling. Int. J. Plasticity 18, 443–459.

Moss, G.L., Pond, R.B., 1975. Inhomogeneous thermal changes in copper during plastic elongation. Metall. Trans. A 6, 1223–1235.

Nesterenko, V.F., Meyers, M.A., Wright, T.W., 1998. Self-organization in the initiation of adiabatic shear bands. Acta Mater. 46, 327–340.

Palik, E.D., 1985. Handbook of Optical Constants. Academic Press, Orlando.

Pina, V., 1997. Mesure de temperature de bande de cisaillement adiabatique dans des alliages de titane. Thesis. University of Paris X, Nanterre.

Piriou, B., 1973. Mise au point sur les facteurs d'émission. Rev. Int. Htes Temp. Réfract. 10, 283–295.

Ranc, N., 2004. Etude des champs de température et de deformation dans les matériaux métalliques sollicités à grande vitesse de deformation. Ph.D. Thesis. University of Paris X.

Ranc, N., Pina, V., Hervé, P., 2000. Optical measurements of phase transition and temperature in adiabatic shear bands in titanium alloy. J. Phys. IV 10, 347–352.

Ranc, N., Pina, V., Sutter, G., Philippon, S., 2004. Temperature measurement by visible pyrometry: orthogonal cutting application. ASME J Heat Transfer 126, 931–936.

Touloukian, Y.S., DeWitt, D.P., 1970. Thermophysical Properties of Matter – Thermal Radiative Properties, vol. 7. IFI/Plenum, New York, Washington.

Tresca, H., 1878. On further application of the flow of solids. Proc. Int. Mech. Engng. 30, 301–345.

Wright, T.W., 2002. The Physics and Mathematics of Adiabatic Shear Bands. Cambridge University Press, Cambridge.

Xue, Q., Meyers, M.A., Nesterenko, V.F., 2002. Self-organization of shear bands in titanium and Ti–6Al–4V alloy. Acta Mater. 50, 575–596.

Zener, C., Hollomon, J.H., 1944. Effect of strain rate upon plastic flow of steel. J. Appl. Phys. 15, 22–32.

Zhou, M., Rosakis, A.J., Ravichandran, G., 1996. Dynamically propagating shear bands in impact-loaded prenotched plates – i. experimental investigations of temperature signatures and propagation speed. J. Mech. Phys. Solids 44 (6), 981–1006.